(23) Siegbahn, P. E. M.; Brandemark, U. B. *Theor. Chim. Acta* **1986**, *69*, 119.

(24) Widmark, P. O.; Roos, B. O. *Theor. Chim. Acta* **1987**, *71*, 411.

(25) Upton, T. H.; Goddard III, W. A. *J. Am. Chem. Soc.* **1978**, *100*, 321.

(26) Akermark, B.; Almemark, M.; Almlof, J.; Backvall, J. E.; Roos, B.; Stogard, A. *J. Am. Chem. Soc.* **1977**, *99*, 4617.

(27) Basch, H.; Newton, M. D.; Moskowitz, J. W. *J. Chem. Phys.* **1978**, *69*, 584.

(28) Itoh, H.; Kunz, A. B. *Chem. Phys. Lett.* **1979**, *66*, 531.

(29) Merle-Mejean, T.; Bouchareb, S.; Tranquille, M. *J. Phys. Chem.* **1989**, *93*, 1197.

(30) Bouchareb, S. Thèse, Université de Bordeaux I, 1983.

(31) Tranquille, M. *Spectra 2000* **1984**, *98*, 43.

(32) Cosse, C. Thèse, Université de Bordeaux I, 1981.

(33) Fischer, K.; Jonas, K.; Wilke, G. *Angew. Chem., Int. Ed. Engl.* **1973**, *12*, 565.

(34) Dekock, R. *Inorg. Chem.* **1971**, *10*, 1205.

(35) Diana, E.; Rossetti, R.; Stanghellini, P. L. *Mater. Chem. Phys.* **1991**, *29*, 333.

(36) Hannachi, Y.; Andrews, L. Manuscript in preparation.

(37) Anson, C. E.; Johnson, B. F. G.; Lewis, J.; Powell, D. B.; Sheppard, N.; Bhattacharyya, A. K.; Bender, B. R.; Bullock, R. M.; Hembre, R. T.; Norton, J. R. *J. Chem. Soc., Chem. Commun.* **1989**, 703.

(38) Jobic, H. *J. Mol. Struct.* **1985**, *131*, 167.

(39) Lehwald, S.; Ibach, H. *Surf. Sci.* **1979**, *89*, 425.

(40) Rosh, N.; Hoffmann, R. *Inorg. Chem.* **1974**, *13*, 2656.

(41) Pitzer, R. P.; Schaefer, H. F. *J. Am. Chem. Soc.* **1979**, *101*, 24.

(42) Green, M.; Howard, J. A. K.; Spencer, J. L.; Stone, F. G. A. *J. Chem. Soc., Chem. Commun.* **1975**, 449.

(43) Kasai, P. H.; McLeod Jr, D.; Watanabe, T. *J. Am. Chem. Soc.* **1980**, *102*, 1.

(44) Kasai, P. H. *J. Phys. Chem.* **1982**, *86*, 19.

(45) Schroeder, W.; Grinter, R.; Schrittenlacher, W.; Rotermund, H. H.; Kolb, D. M. *J. Chem. Phys.* **1985**, *82*, 1623.

(46) Arnold, B. R.; Balaji, V.; Michl, J. *J. Am. Chem. Soc.* **1990**, *112*, 1808.

(47) Grogan, M. J.; Nakamoto, K. *Inorg. Chim. Acta* **1967**, *1*, 228.

(48) Nishihara, H.; Fujita, M.; Takahashi, H.; Saito, T.; Sasaki, Y. *Transition Met. Chem.* **1980**, *5*, 98.

(49) Jonas, K.; Heimbach, P.; Wilke, G. *Angew. Chem., Int. Ed. Engl.* **1969**, *7*, 949.

(50) Ozin, G. A.; Power, W. J. *Inorg. Chem.* **1980**, *19*, 3860.

(51) Arnold, B. R.; Balaji, V.; Downing, J. W.; Radziszewski, J. G.; Fisher, J. J.; Michl, J. *J. Am. Chem. Soc.* **1991**, *113*, 2910.

Resolution of the Properties of Hydrogen-Bonded Tyrosine Using a Trilinear Model of Fluorescence

Jin Keun Lee, Robert T. Ross,* Satheesh Thampi, and Sue Leurgans[†]

Biophysics Program, Department of Biochemistry, and Department of Statistics, The Ohio State University, Columbus, Ohio 43210 (Received: May 15, 1992; In Final Form: July 31, 1992)

The fluorescence of any dilute specimen is separately linear in functions of each of the independent variables excitation wavelength, emission wavelength, and any treatment which alters concentration or fluorescence quantum yield. The resulting trilinear models have a structure that permits the mathematical dissection of spectra from complex specimens without the use of any other information about the properties of the specimen. Using this technique, the steady-state fluorescence at aqueous *N*-acetyl-L-tyrosinamide in the presence of five proton acceptors was resolved into three components, corresponding to normally solvated side chain, side chain hydrogen-bonded to the added proton acceptor, and impurity. The excitation spectrum of the hydrogen-bonded complex is red-shifted about 2 nm. The emission maximum of the complex is 310 nm for phosphate monoanion, 320 nm for acetate, 330 nm for phosphate bianion, and 335 nm for imidazole and tris(hydroxymethyl)aminomethane. All binding constants for complex formation and reciprocal quenching constants for fluorescence are between 0.2 and 0.3 M, except for phosphate monoanion, for which both constants are 3.3 M. The temperature dependence of the binding constants is small, giving a ΔH for complex dissociation between −0.8 and 0.0 kcal/mol.

Introduction

The hydroxyl group of tyrosine ionizes to produce tyrosinate with a pK_a of about 10 in the ground state[1,2] and an estimated pK_a of 4–5 in the excited state.[3] Ground-state tyrosinate has an absorption maximum at 295 nm, an emission maximum at 345 nm, and a fluorescence quantum yield which is about 10 times less than that of tyrosine.[1,4] Tyrosinate formed in the excited state has not been well characterized because the rate of deactivation by emission is much faster than the rate of ionization.[5]

Quenching effects of acetate and phosphate on tyrosine fluorescence have been shown in model compound systems[5-8] as well as in proteins.[9] The quenching effect of amines on phenols[10,11] implies a possible quenching by amine groups on tyrosine.

The ionization of excited-state tyrosine by proton transfer from tyrosine to the proton acceptor has been proposed to interpret a second emission band that accompanies the quenching effect.[3,7,8,12] The excited-state tyrosinate whose formation was facilitated by a proton acceptor was described as having the same emission maximum as ground-state tyrosinate. However, Willis and Szabo[13] have recently shown that the emission maximum varies between that of ground-state tyrosine (305 nm) and that of tyrosinate (345 nm), depending on the proton acceptor. They propose that the observed emission is from a hydrogen-bonded complex formed in the ground state between tyrosine and the proton acceptor, rather than from tyrosinate formed in the excited state by proton transfer.

In proteins, tyrosine residues are often hydrogen bonded with the carboxylate group of aspartate and glutamate residues, and with the carbonyl group of main chains.[14] Several tyrosine-containing proteins with no tryptophan have been reported to have an emission maximum in the range of 315–350 nm.[15-21] More recently, hydrogen bonding between phosphate bianion and tyrosine residues in a DNA-stabilizing protein has been shown to have an important role in protein–nucleic acid binding.[9] Therefore, knowledge of the properties of hydrogen-bonded tyrosine is very important in understanding protein fluorescence.

N-Acetyl-L-tyrosinamide (NAYA) has been widely used as a model compound for a tyrosine residue in proteins. It is a simpler model than tyrosine in studies of ionization properties because it has both the amino and carboxyl groups blocked.[2,4,8,12,22,23]

In this work the steady-state fluorescence of NAYA in aqueous solutions containing different concentrations (0.005–2.5 M) of a proton acceptor, or at different pH values (pH 8.0–10.5), has been studied by trilinear analysis. The proton acceptors used were

---

* To whom correspondence should be addressed, at the Department of Biochemistry, 484 West 12th Ave.

[†] Present address: Department of Preventive Medicine, Rush-Presbyterian-St. Luke's Medical Center, 1725 W. Harrison St., Suite 117, Chicago, IL 60612.

0022-3654/92/2096-9158$03.00/0

five of those investigated by Willis and Szabo,[13] who selected them to represent possible hydrogen-bond partners for tyrosine residues in proteins.

The trilinear model used is known as PARAFAC.[24-27] This trilinear model is an extension of the bilinear models that have been used in spectroscopy, sometimes under the name *factor analysis*.[28,29] The utility of bilinear models is often limited because the parameter vectors (such as spectra) that they yield are not unique; rather, the data can be fit equally well with linear combinations of the vectors initially obtained. Extra information is necessary to fix these linear combinations.[30] A major advantage of the PARAFAC trilinear model is that the indeterminacy of bilinear models is usually absent.[26,30] Several spectroscopic studies using trilinear models have been reported.[31-39]

In recent years, many fluorescence spectroscopists have taken a different approach to data analysis: Fluorescence intensity is measured using two independent variables, such as emission wavelength and time. The data are then fit with a bilinear model, with the dependence on one variable, usually time, described by a specific equation having two to four parameters for each component.[40-43] Quencher concentration has also been used as the variable for which there is a specific equation.[44-46] This approach, which is often called *global analysis*, usually avoids the linear-combination indeterminacy of a general bilinear model by using a sufficiently specific model for one variable, such as a sum of two exponentials for dependence on time. The advantage of the general multilinear model used in this report is that the observable need not depend on any independent variable according to a functional form that is specified in advance.

The fluorescence of a dilute specimen is separately linear in functions of each of the independent variables: excitation wavelength, emission wavelength, concentration, and any chemical treatment which alters fluorescence quantum yield. Hence, we have the equation

$$\mu_{ijkl} = \sum_{f=1}^{F} \epsilon_f(\lambda_i)\ \pi_f(\lambda_j)\ c_f(k)\ \phi_f(l) \qquad (1)$$

where ϵ is the relative absorbance of component f at excitation wavelength i, π is the relative fluorescence intensity of f at emission wavelength j, c is the concentration of f, and ϕ is the relative fluorescence yield of f. In the experiments described here, both concentration and fluorescence quantum yield are affected by a single independent variable, the concentration of a proton acceptor. Hence, the last two terms are combined, giving the trilinear equation

$$\mu_{ijk} = \sum_{f=1}^{F} \epsilon_f(\lambda_i)\ \pi_f(\lambda_j)\ \phi_f([\mathrm{A}]_k) \qquad (2)$$

where ϕ is the relative fluorescence yield of component f at proton acceptor concentration $[\mathrm{A}]_k$.

Experimental Section

All water was obtained from a Millipore Milli-Q UV Plus system, which uses UV irradiation to supplement a cartridge system in removing organic contaminants. Imidazole (Matheson, Coleman, and Bell) was dissolved in ethanol (HPLC grade, Fisher), treated with activated charcoal, filtered, recrystallized, dissolved in water, and passed through two cycles of treatment with activated charcoal followed by filtration. Potassium chloride (Fisher), sodium acetate (HPLC grade, Fisher), potassium phosphate, dibasic (Mallinckrodt), and tris(hydroxymethyl)-aminomethane (Tris, Sigma) were each dissolved in water and purified by four cycles of charcoal treatment. Boric acid (Mallinckrodt) and potassium carbonate (Mallinckrodt) were purified by a cycle of charcoal treatment.

Specimens measured were 0.025 mM in NAYA (Aldrich) and were 0.5 M in KCl to reduce the variation of ionic strength of the solutions. The pH used with each proton acceptor was chosen to be the same as that used by Willis and Szabo,[13] who had picked the pH to provide as much as possible of the desired ionization state of the proton acceptor, while staying much lower than the pK_a of the ground-state ionization of the phenol side chain to minimize the formation of the ground-state anion. NAYA in 0.01 M borate (pH 8.0–9.5) or 0.01 M carbonate (pH 10.0–11.5) was used to study the formation of ground-state anion.

Fluorescence data collection was performed using 19 excitation wavelengths (260–290 nm) and 20 emission wavelengths (290–400 nm) for 6 different concentrations (0.005–2.5 M) of each proton acceptor at 26, 31, and 36 °C, and using 13 excitation wavelengths (260–310 nm) and 20 emission wavelengths (290–400 nm) for 8 different pH values (pH 8–11.5) at 26 °C. Excitation and emission band passes were each 2 nm. Calibration of the spectral sensitivity of the SLM SPF-500C spectrofluorometer (SLM Instruments, Urbana, IL) was carried out using standard compounds.[47-49] All data were corrected for background signal by subtraction of a blank that was identical to the specimen except for the absence of added NAYA.

The corrected data were transferred to a supercomputer and fit by weighted nonlinear least squares to the trilinear model described by eq 2, with the parameters constrained to be nonnegative. The data set for each proton acceptor and temperature, as well as for the pH titration experiment, was fit with models having one, two, and three components. The three-component model ($F = 3$) was used to separate impurity fluorescence from the two components of interest. The code uses an accelerated adaptation of the alternating-least-squares algorithm,[50] with the decomposition of Leurgans et al.[51] used to obtain a starting solution for $F > 1$.

Results

Sixteen datasets, fifteen of them corresponding to five proton acceptors at three temperatures, and one of them for the pH dependence of anion formation, were collected and analyzed independently.

Resolution of Fluorescence in the Presence of Proton Acceptors. An example of the resolution obtained by fitting a three-component model is shown in Figure 1. The estimated fluorescence from a component at a specific excitation wavelength, emission wavelength, and proton acceptor concentration is the product of the corresponding points on the three graphs. The excitation and emission spectra for the three components have been normalized to have a maximum fluorescence intensity of 1.0. The relative fluorescence intensity of the three components at each specific concentration of proton acceptor is shown in the third graph.

In all fifteen cases, a component was observed with an excitation maximum of 274 nm and an emission maximum of 302 nm which was gradually quenched with increasing concentration of the proton acceptor. All characteristics of this component are consistent with its identity as normally solvated NAYA. In all cases, a second component was observed with a slightly red-shifted excitation spectrum (Figure 2, top) and an emission maximum between 309 and 336 nm, depending on the proton acceptor (Figure 2, bottom), whose fluorescence intensity gradually increased with increasing concentration of the proton acceptor. The characteristics of this component are consistent with its identity as NAYA whose side chain is hydrogen-bonded to the added proton acceptor. In all cases, the weakest of three components had a broad excitation spectrum peaking near 290 nm and a broad emission maximum peaking near 400 nm; it increased with increasing concentration of NAYA (data not shown). The characteristics of this component suggest that it is impurity, primarily associated with NAYA.

After eq 2 had been fit to each data set, an appropriate model for the parameters describing relative fluorescence intensity for the different concentrations of the proton acceptor was fit by least squares. The Stern–Volmer quenching equation was fit to the normal NAYA component and the equation for the formation of a 1:1 hydrogen-bonded complex to the second component (see Figure 1).

The results of the analysis of the fifteen data sets are summarized in Table I. The parameters ϕ_1 and ϕ_2 are the relative intensities of fluorescence of the first and second components at their respective excitation and emission maxima. The column

TABLE I: Properties of Hydrogen-Bonded Tyrosine Fluorescence in Aqueous Solution

proton acceptor	pK_a	pH	T, °C	λ_{max},[a] nm	ϕ_2/ϕ_1[b]	$1/K_{SV}$,[c] M	K_D,[d] M	ΔH,[e] kcal/mol
phosphate[f]	2.15	4.5	26	309	0.0549 ± 0.0090	3.321 ± 0.491	3.360 ± 0.847	−0.78 ± 0.40
			31	310	0.0552 ± 0.0059	3.306 ± 0.289	3.227 ± 0.538	
			36	309	0.0570 ± 0.0077	3.294 ± 0.288	3.221 ± 0.684	
acetate	4.77	6.0	26	319	0.0746 ± 0.0003	0.213 ± 0.007	0.295 ± 0.027	−0.07 ± 0.09
			31	320	0.0768 ± 0.0003	0.197 ± 0.011	0.296 ± 0.019	
			36	320	0.0770 ± 0.0003	0.186 ± 0.011	0.294 ± 0.024	
imidazole	6.99	7.5	26	335	0.0433 ± 0.0002	0.196 ± 0.018	0.206 ± 0.025	−0.66 ± 0.23
			31	334	0.0428 ± 0.0002	0.189 ± 0.021	0.200 ± 0.027	
			36	335	0.0441 ± 0.0003	0.193 ± 0.020	0.198 ± 0.022	
phosphate[g]	7.20	8.0	26	327	0.1937 ± 0.0009	0.242 ± 0.013	0.285 ± 0.029	−0.28 ± 0.07
			31	329	0.1894 ± 0.0008	0.233 ± 0.019	0.283 ± 0.025	
			36	330	0.1916 ± 0.0008	0.219 ± 0.015	0.280 ± 0.028	
Tris[h]	8.36	8.0	26	335	0.0528 ± 0.0003	0.272 ± 0.012	0.279 ± 0.024	−0.45 ± 0.10
			31	335	0.0575 ± 0.0003	0.268 ± 0.017	0.276 ± 0.020	
			36	336	0.0551 ± 0.0004	0.263 ± 0.013	0.272 ± 0.023	

[a] Wavelength of maximum emission. [b] Ratio of the relative fluorescence intensity of the second component to the first component at their respective excitation and emission maxima. [c] Stern–Volmer constant for quenching NAYA. [d] Dissociation constant of the hydrogen-bonded NAYA complex. [e] ΔH for complex dissociation, calculated using K_D to higher precision than shown in this table. [f] Phosphate monoanion. [g] Phosphate bianion. [h] Tris(hydroxymethyl)aminomethane.

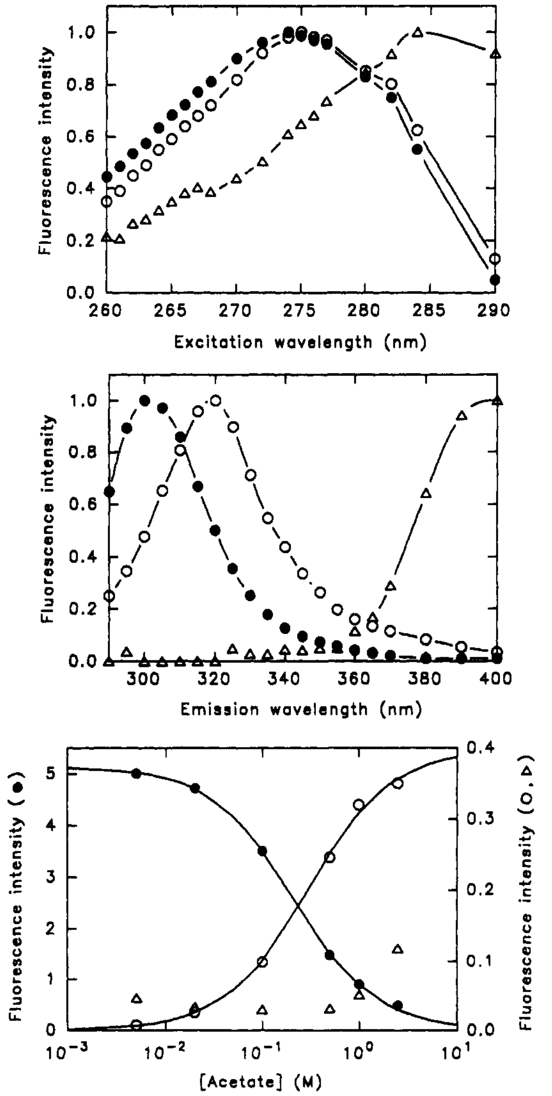

Figure 1. Resolution of fluorescence of NAYA in acetate at 26 °C into three components, corresponding to normal NAYA (●), NAYA–acetate complex (○), and impurity (△). The solid lines in the [acetate]-dependence graph are least-squares fits of the equations for Stern–Volmer quenching and 1:1 complex formation.

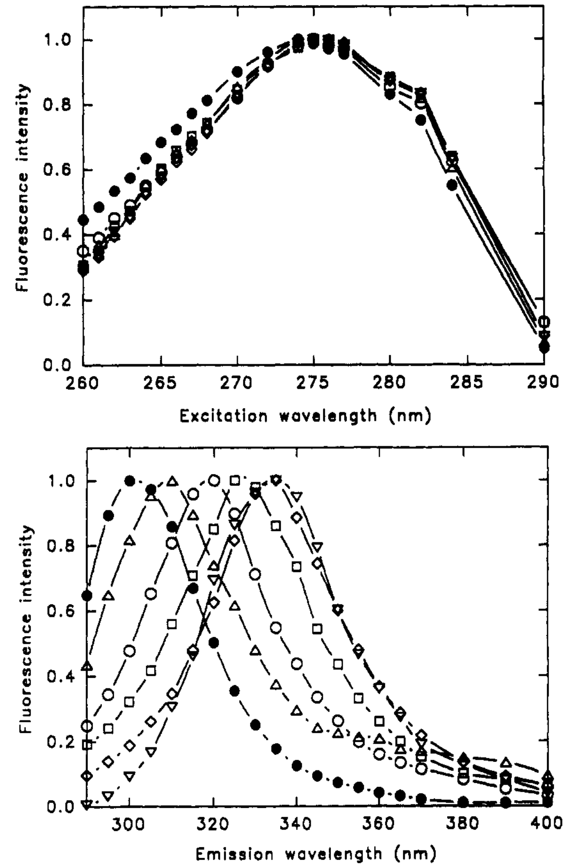

Figure 2. Excitation and emission spectra of normal NAYA (●) and of NAYA hydrogen-bonded to phosphate monoanion (△), acetate (○), imidazole (▽), phosphate bianion (□), and Tris (◇) at 26 °C.

$1/K_{SV}$ is the reciprocal of the Stern–Volmer quenching constant. The column K_D is the dissociation constant of the hydrogen-bonded complex. Values of ΔH were obtained by linear regression of ln (K_D) versus $1/T$. In all cases, the deduced parameters are those for the mixture of ionic species present under the conditions of the experiment. The errors are asymptotic based on assuming constant variance in the points modeled. Therefore, the standard errors shown may be over- or underestimates and are very approximate.

Both $1/K_{SV}$ and K_D are in the range of 0.2 and 0.3 M in all cases except phosphate monoanion, whose $1/K_{SV}$ and K_D are about 3.3 M. When K_D and $1/K_{SV}$ are the same, quenching is probably due solely to static quenching upon complex formation. A K_D larger than $1/K_{SV}$ suggests that there is also a second, dynamic, quenching process. For the phosphate mono- and bianions, imidazole, and Tris, K_D is not statistically significantly larger than $1/K_{SV}$ (P = 0.52, 0.053, 0.39, 0.39; z-test). For acetate, K_D is larger than $1/K_{SV}$ ($P < 0.001$).

The effect of temperature on the spectra for acetate is shown in Figure 3. The temperature dependence of both the quenching

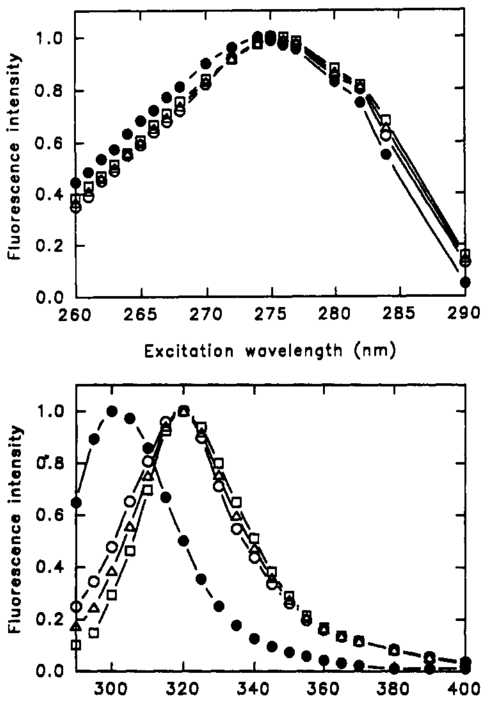

Figure 3. Temperature effect on the fluorescence properties of hydrogen-bonded NAYA in acetate at 26 °C (○), 31 °C (△), and 36 °C (□). The solid circle is for the normal NAYA component.

and the binding constants is small, and the ΔH for complex dissociation is close to zero.

Resolution of Fluorescence of Anion. Equation 2 was fit to a data set with pH as the chemical variable. The resolution is shown in Figure 4. Normal NAYA was observed with an excitation maximum at 274 nm and an emission maximum at 305 nm. The anion was observed with an excitation maximum at 295 nm and an emission maximum at 343 nm. Impurity was observed with an excitation maximum at 310 nm and an emission maximum at 400 nm; its spectra were similar to those of the impurity found in the presence of proton acceptors, and its fluorescence intensity increased at high pH. The characteristics of this impurity are very similar to those of bityrosine,[52] which is the *o*,*o*-biphenol analog of tyrosine. Bityrosine produced by UV irradiation has an excitation maximum of 315 nm and an emission maximum of 405 nm, and its absorption at 315 nm increases at higher pH.

The Henderson–Hasselbalch equation was fit to the relative fluorescence intensity at different pH values, yielding a ground-state pK_a of the hydroxyl group of NAYA of 9.89 ± 0.03.

Discussion

Excited-state proton transfer from tyrosine to the proton acceptor has often been employed to interpret the quenching effect of acetate and phosphate bianion on tyrosine.[3,7,8] However, confirming the results of Willis and Szabo,[13] we have observed that the emission maximum of the "tyrosinate" component varies between that of tyrosine and that of ground-state tyrosinate, depending on the proton acceptor, and is red-shifted in proportion to the pK_a of the proton acceptor.

Our emission maxima for complexes with acetate, imidazole, phosphate bianion, and Tris agree with those found by Willis and Szabo. In addition, we have been able to measure the emission from the complex with phosphate monoanion and to determine binding constants for all of the complexes studied.

In previous work, the quenching constants K_{SV} for tyrosine by acetate,[3] phosphate monoanion, and phosphate bianion[8] have been determined to be 5.7, 1.5, and 5.0 M^{-1}, respectively. NAYA has been reported to have a K_{SV} of 0.75 and 3.9 M^{-1} for phosphate monoanion and bianion, respectively.[8] Our values of K_{SV} for NAYA by acetate, phosphate monoanion, and phosphate bianion at 26 °C are 4.7, 0.30, and 4.1 M^{-1}, respectively. Our estimated binding constant for phosphate bianion is 3.5 M^{-1}, which is much higher than the association constant of 0.5 M^{-1} from UV absorption difference spectra.[8]

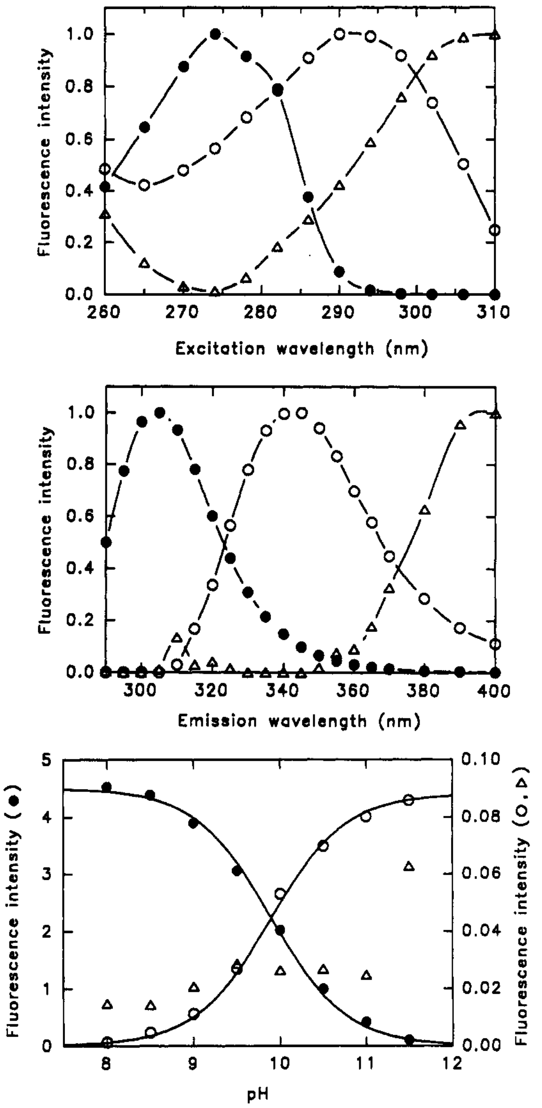

Figure 4. Resolution of fluorescence of NAYA at 26 °C into three components, corresponding to normal NAYA (●), ground-state anion (○), and impurity (△). The solid lines in the pH-dependence graph are least-squares fits of the Henderson–Hasselbalch equation.

For acetate, the binding constant is greater than the quenching constant, indicating that there is not only a static quenching upon complex formation but also a second, dynamic, quenching process. For the other proton acceptors, the binding constants are not significantly greater than their quenching constants.

The ability of trilinear modeling of steady-state fluorescence data to provide the results reported here suggests that this technique will be generally useful in resolving the properties of minor components in mixtures of fluorophores. The resolution of tyrosines in different hydrogen-bonded environments in a protein may be a particularly important application.

Acknowledgment. This research was supported by grants from the National Science Foundation (DMS88-05402 and DMS89-02265) and from the Ohio Supercomputer Center. We thank W. J. Becktel and E. J. Behrman for helpful discussions. We also thank D. L. North for developing a fluorescent impurity purification method.

References and Notes

(1) Cornog, J. L.; Adams, W. R. *Biochim. Biophys. Acta* **1963**, *66*, 356.
(2) Liu, X.-Y.; Cottrell, K. O.; Nordlund, T. M. *Photochem. Photobiol.* **1989**, *50*, 721.
(3) Rayner, D. M.; Krajcarski, D. T.; Szabo, A. G. *Can. J. Chem.* **1978**, *56*, 1238.

(4) Longworth, J. W. *Biochim. Biophys. Acta* **1967**, *147*, 526.
(5) Feitelson, J. *J. Phys. Chem.* **1964**, *68*, 391.
(6) Chen, R. F.; Cohen, P. F. *Arch. Biochem. Biophys.* **1966**, *114*, 514.
(7) Shimizu, O.; Watanabe, J.; Imakubo, K. *Photochem. Photobiol.* **1979**, *29*, 915.
(8) Alev-Behmoaras, T.; Toulme, J.; Helene, C. *Photochem. Photobiol.* **1979**, *30*, 533.
(9) Searcy, D. G.; Montenay-Garestier, T.; Laston, D. J.; Hélène, C. *Biochim. Biophys. Acta* **1988**, *953*, 321.
(10) Scott, R. M.; DePalma, O.; Vinogradov, S. N. *J. Phys. Chem.* **1968**, *72*, 3192.
(11) Bisht, P. B.; Tripathi, H. B.; Pant, D. D. *J. Lumin.* **1989**, *43*, 301.
(12) Schnarr, M.; Hélène, C. *Photochem. Photobiol.* **1982**, *36*, 91.
(13) Willis, K. J.; Szabo, A. G. *J. Phys. Chem.* **1991**, *95*, 1585.
(14) Baker, E. N.; Hubbard, R. E. *Prog. Biophys. Mol. Biol.* **1984**, *44*, 97.
(15) Graziani, M. T.; Agro, A. F.; Rotilio, G.; Barra, D.; Mondovi, B. *Biochemistry* **1974**, *13*, 804.
(16) Szabo, A. G.; Lynn, K. R.; Krajcarski, D. T.; Rayner, D. M. *FEBS Lett.* **1978**, *94*, 249.
(17) Lim, B. T.; Kimura, T. *J. Biol. Chem.* **1980**, *255*, 2440.
(18) Longworth, J. W. *Ann. N.Y. Acad. Sci.* **1981**, *366*, 237.
(19) Jordano, J.; Barbero, J. L.; Montero, F.; Franco, L. *J. Biol. Chem.* **1983**, *258*, 315.
(20) Pundak, S.; Roche, R. S. *Biochemistry* **1984**, *23*, 1549.
(21) O'Neil, J. D. J.; Hofmann, T. *Biochem. J.* **1987**, *243*, 611.
(22) Follenius, A.; Gérard, D. *Photochem. Photobiol.* **1983**, *38*, 373.
(23) Lux, B.; Baudier, J.; Gérard, D. *Photochem. Photobiol.* **1985**, *42*, 245.
(24) Carroll, J. D.; Chang, J.-J. *Psychometrika* **1970**, *35*, 283.
(25) Harshman, R. A. *UCLA Working Papers in Phonetics* **1970**, *16*, 1.
(26) Law, H. G.; Snyder, C. W., Jr.; Hattie, J. A.; McDonald, R. P. *Research Methods for Multimode Data Analysis*; Praeger: New York, 1984.
(27) Leurgans, S.; Ross, R. T. *Stat. Sci.* **1992**, *7*, 289.
(28) Malinowski, E. R.; Howery, D. G. *Factor Analysis in Chemistry*; Wiley-Interscience: New York, 1980.
(29) Hofrichter, J.; Sommer, J. H.; Henry, E. R.; Eaton, W. A. *Proc. Natl. Acad. Sci. U.S.A.* **1983**, *80*, 2235.
(30) Kruskal, J. B. *Proc. Symp. Appl. Math.* **1983**, *28*, 75.
(31) Appellof, C. J.; Davidson, E. R. *Anal. Chem.* **1981**, *53*, 2053.
(32) Callis, J. B. In *Ultrahigh Resolution Chromatography*; Ahuja, S., Ed.; American Chemical Society Symposium Series No. 250; American Chemical Society: Washington, DC, 1984.
(33) Russell, M. D.; Gouterman, M. *Spectrochim. Acta* **1988**, *44A*, 857.
(34) Russell, M. D.; Gouterman, M. *Spectrochim. Acta* **1988**, *44A*, 863.
(35) Russell, M. D.; Gouterman, M.; Van Zee, J. A. *Spectrochim. Acta* **1988**, *44A*, 873.
(36) Burdick, D. S.; Tu, X. M.; McGown, L. B.; Millican, D. W. *J. Chemom.* **1990**, *4*, 15.
(37) Durell, S. R.; Lee, C.-H.; Ross, R. T.; Gross, E. L. *Arch. Biochem. Biophys.* **1990**, *278*, 148.
(38) Lee, C.-H.; Kim, K.; Ross, R. T. *Korean Biochem. J.* **1991**, *24*, 374.
(39) Ross, R. T.; Lee, C.-H.; Davis, C. M.; Ezzeddine, B. M.; Fayyad, E. A.; Leurgans, S. E. *Biochim. Biophys. Acta* **1991**, *1056*, 317.
(40) Knutson, J. R.; Beechem, J. M.; Brand, L. *Chem. Phys. Lett.* **1983**, *102*, 501.
(41) Alcala, R.; Gratton, E. J.; Prendergast, F. G. *Biophys. J.* **1987**, *51*, 925.
(42) Willis, K. J.; Szabo, A. G.; Drew, J.; Zuker, M.; Ridgeway, J. M. *Biophys. J.* **1990**, *57*, 183.
(43) Beechem, J. M.; Gratton, E.; Ameloot, M.; Knutson, J. R.; Brand, L. In *Topics in Fluorescence Spectroscopy*; Lakowicz, J. R., Ed.; Plenum Press: New York, 1991; Vol. 2.
(44) Stryjewski, W.; Wasylewski, Z. *Eur. J. Biochem.* **1986**, *158*, 547.
(45) Wasylewski, Z.; Koloczek, H.; Wasniowska, A. *Eur. J. Biochem.* **1988**, *172*, 719.
(46) Eftink, M. R.; Wasylewski, Z. *Biochemistry* **1989**, *28*, 382.
(47) Berlman, I. B. *Handbook of Fluorescence Spectra of Aromatic Molecules*, 2nd ed.; Academic Press: New York, London, 1971.
(48) Melhuish, W. H. *Appl. Opt.* **1975**, *14*, 26.
(49) Madge, D.; Brannon, J. H.; Cremers, T. L.; Olmsted, J., III. *J. Phys. Chem.* **1979**, *83*, 696.
(50) Sands, R.; Young, F. W. *Psychometrika* **1980**, *45*, 39.
(51) Leurgans, S. E.; Ross, R. T.; Abel, R. B. *SIAM J. Matrix Anal.*, in press.
(52) Lehrer, S. S.; Fasman, G. D. *Biochemistry* **1967**, *6*, 757.

IR Photodissociation and Collision Induced Dissociation Study of Ethene Cluster Ions

Thomas N. Feinberg, Tomas Baer,* and Liam M. Duffy

Department of Chemistry, University of North Carolina, Chapel Hill, North Carolina 27599
(Received: May 28, 1992; In Final Form: August 3, 1992)

Clusters of ethene ions were produced by electron impact of a supersonic expansion of 5% ethene in argon. Significant cluster ion formation could be obtained only by ionizing at the nozzle orifice. Mass-selected ions were then photodissociated by the absorption of a single photon from a CW CO_2 laser. The products were mass and energy analyzed by an electric sector. Dissociation by collisions with the slit of the electric sector gave collision induced dissociation (CID) spectra. Of the many ions produced in the source, eight of them could be photodissociated with the low-energy (120 meV) CO_2 laser photons. These ions, once excited, dissociated rapidly with a lifetime less than 10^{-7} s. Proposed structures for all but one of these ions consist of an even-electron stable core ion surrounded by one to three ethene molecules. The stable core ions are $C_3H_3^+$ (m/z 39), $C_3H_5^+$ (m/z 41), $C_4H_9^+$ (m/z 57), and $C_6H_{11}^+$ (m/z 83). Modeling of these dissociation reactions with the statistical theory (RRKM) suggests that the ethene units are bound weakly to these ions. The only odd-electron ion that could be photodissociated had the nominal mass of the tetramer of ethene (m/z 112).

I. Introduction

Ion–molecule reactions involving ethene have been conducted for several decades using mass spectrometers, high-pressure mass spectrometers, and ion beam machines. A landmark paper on chemical ionization by Field et al.[1] first investigated the products of ethene ion addition to neutral ethene. From this work and subsequent reports,[2,3] they found that the high molecular weight ions observed in the mass spectrum were indicative of fast reactions between neutral ethene and the ions formed by electron impact (EI). Experiments by Kebarle et al.[4-7] and Wexler and Marshall[8] found marked differences in the relative yields of these larger polyatomic species when using argon/ethene versus xenon/ethene mixtures. The occurrence of these high molecular weight ions led all of these investigators to suggest that an ionic polymerization mechanism was responsible for the formation of these hydrocarbons.

The recent addition of cluster beam sources has added a new dimension to these studies.[9,10] Ionization of neutral ethene clusters provides a different initial condition for the formation of the ion–molecule products than the two or three body collisions dominant in a high-pressure ion source. Comparisons between the chemistries within these ionic clusters and the reactions found in a high-pressure ion source have found that, for many cluster ions, the dissociation pathway proceeds through a common molecular ion geometry.[11,12]

The isomerization between different configurations of $C_6H_{12}^+$ has been examined by Tzeng et al.[11,12] They found similarities between the relative abundances of fragment ions from the ethene

0022-3654/92/2096-9162$03.00/0